

High efficiency sub-nanosecond electro-optical *Q*-switched laser operating at kilohertz repetition frequency

Xin Zhao(赵鑫), Zheng Song(宋政), Yuan-Ji Li(李渊骥), Jin-Xia Feng(冯晋霞), Kuan-Shou Zhang(张宽收)
Citation: Chin. Phys. B . 2020, 29(8): 084205 . **doi:** 10.1088/1674-1056/ab8ac4
Journal homepage: http://cpb.iphy.ac.cn; http://iopscience.iop.org/cpb

What follows is a list of articles you may be interested in

Influences of annealing temperature on properties of Fe^{2+}: ZnSe thin films deposited by electron beam evaporation and their applications to *Q*-switched fiber laser

Du-Xin Qing(卿杜鑫), Shu-Tong Wang(王树同), Shou-Gui Ning(宁守贵), Wei Zhang(张伟), Xiao-Xu Chen(陈晓旭), Hong Zhang(张弘), Guo-Ying Feng(冯国英), Shou-Huan Zhou(周寿桓)
Chin. Phys. B . 2020, 29(5): 054208 . **doi:** 10.1088/1674-1056/ab81f2

Passively *Q*-switched diode-pumped Tm, Ho: $LuVO_4$ laser with a black phosphorus saturable absorber

Linjun Li(李林军), Tianxin Li(李天鑫), Long Zhou(周龙), Jianying Fan(范剑英), Yuqiang Yang(杨玉强), Wenqiang Xie(谢文强), Shasha Li(李莎莎)
Chin. Phys. B . 2019, 28(9): 094205 . **doi:** 10.1088/1674-1056/ab33f1

Correction of walk-off-induced wavefront distortion for continuous-wave laser

Hongxin Zou(邹宏新), Guozhu Chen(陈国柱), Yue Wu(伍越), Yong Shen(沈咏), Qu Liu(刘曲)
Chin. Phys. B . 2016, 25(9): 094211 . **doi:** 10.1088/1674-1056/25/9/094211

33 W quasi-continuous-wave narrow-band sodium D_{2a} laser by sum-frequency generation in LBO

Wang Peng-Yuan, Xie Shi-Yong, Bo Yong, Wang Bao-Shan, Zuo Jun-Wei, Wang Zhi-Chao, Shen Yu, Zhang Feng-Feng, Wei Kai, Jin Kai, Xu Yi-Ting, Xu Jia-Lin, Peng Qin-Jun, Zhang Jing-Yuan, Lei Wen-Qiang, Cui Da-Fu, Zhang Yu-Dong, Xu Zu-Yan
Chin. Phys. B . 2014, 23(9): 094208 . **doi:** 10.1088/1674-1056/23/9/094208

A picosecond widely tunable deep-ultraviolet laser for angle-resolved photoemission spectroscopy

Zhang Feng-Feng, Yang Feng, Zhang Shen-Jin, Xu Zhi, Wang Zhi-Min, Xu Feng-Liang, Peng Qin-Jun, Zhang Jing-Yuan, Wang Xiao-Yang, Chen Chuang-Tian, Xu Zu-Yan
Chin. Phys. B . 2013, 22(6): 064212 . **doi:** 10.1088/1674-1056/22/6/064212

High efficiency sub-nanosecond electro–optical Q-switched laser operating at kilohertz repetition frequency*

Xin Zhao(赵鑫)[1], Zheng Song(宋政)[1], Yuan-Ji Li(李渊骥)[1,2,†], Jin-Xia Feng(冯晋霞)[1,2], and Kuan-Shou Zhang(张宽收)[1,2]

[1] *State Key Laboratory of Quantum Optics and Quantum Optics Devices, Institute of Opto-Electronics, Shanxi University, Taiyuan* 030006, *China*
[2] *Collaborative Innovation Center of Extreme Optics, Shanxi University, Taiyuan* 030006, *China*

(Received 29 February 2020; revised manuscript received 23 March 2020; accepted manuscript online 18 April 2020)

Based on a theoretical model of Q-switched laser with the influences of the driving signal sent to the Pockels cell and the doping concentration of the gain medium taken into account, a method of achieving high energy sub-nanosecond Q-switched lasers is proposed and verified in experiment. When a Nd:YVO_4 crystal with a doping concentration of 0.7 at.% is used as a gain medium and a driving signal with the optimal high-level voltage is applied to the Pockels cell, a stable single-transverse-mode electro–optical Q-switched laser with a pulse width of 0.77 ns and a pulse energy of 1.04 mJ operating at the pulse repetition frequency of 1 kHz is achieved. The precise tuning of the pulse width is also demonstrated.

Keywords: milijoule level sub-nanosecond laser, kilohertz repetition frequency, doping concentration of laser crystal, tunable pulse width

PACS: 42.60.By, 42.60.Gd **DOI:** 10.1088/1674-1056/ab8ac4

1. Introduction

Solid state lasers with kilohertz (kHz) level pulse repetition frequency (PRF), sub nanosecond (ns) pulse width (PW), and pulse energy higher than 1 milijoule (mJ) are very attractive for a variety of applications, such as laser ranging, microprocessing, nonlinear frequency conversion, photoacoustic imaging, surface physics, and material science.[1–8]

Many techniques, including electro–optical (EO) Q-switching, passive Q-switching using saturable absorber,[9,10] mode-locking,[11] and stimulated Brillouin scattering (SBS),[12] can be used to build the lasers with PW at ns or picosecond level. In comparison with the others, EO Q-switched lasers have a lot of advantages, *e.g.*, better controllability, easy-to-realize synchronization, high stability and reliability, *etc*. A feasible method of shortening the PW of an EO Q-switched laser operating at kHz PRF is to reduce the cavity length by employing small-scaled gain medium and Q switch. Zayhowski and Dill demonstrated a coupled-cavity EO Q-switched laser with a cavity length of 1.34 mm producing 12-μJ pulses of 115-ps duration at 1-kHz PRF.[13] However, the pulse energy of this kind of laser was excessively low due to the poor absorbed pump energy. Horiuchi *et al.* presented an alternative method by using an EO deflector,[14] a pulse laser with 100-kHz PRF, nearly 0.02-mJ pulse energy and 6.4-ns PW was obtained due to the short cavity length and the high speed of loss switching of the deflector. Another method frequently used to build EO Q-switched lasers with short PW is to employ output coupler (OC) with high transmission. Liu *et al.* reported a side-pumped EO Q-switched pulse laser with 1-kHz PRF, 1.15-mJ pulse energy, and 1.3-ns PW at the equivalent output transmission of 80% and peak pump power as high as 100 W.[15] In this case, the pump power should be very high, so high that it exceeds the pump threshold and reaches a high gain-to-loss ratio, but high energy consumption and problems such as serious thermal effects of gain medium and thermal induced depolarization of Pockels cell (PC) may take place and need solving.[16,17] Besides the cavity length and OC transmission, the PRF is also an important factor that influences the PWs of lasers. Usually, the pulse buildup time and duration will be increased when the laser operates at higher PRF. One way to circumvent this problem is to use the technique of cavity dumped Q-switching with the advantage that high PRF and enhanced pulse energy can be obtained simultaneously. McDonagh *et al.* demonstrated a 0.94-mJ cavity dumped Q-switched single-transverse-mode (TEM_{00}) laser with a pulse width of 6 ns at 50-kHz PRF.[18] Liu *et al.* reported a pulse width adjustable Q-switched cavity dumped Nd:YVO_4 laser with a pulse width adjustment range of 4.8 ns–7.8 ns at 10-kHz PRF by rotating an intracavity quarter-wave plate (QWP) and PC.[19] Another method named as active-passive Q-switching was also proposed and employed to narrow the pulse width of lasers at high PRF. Using both a β-BaB_2O_4 (BBO) EO modulator and a GaAs saturable absorber, Li *et al.* demonstrated a doubly Q-switched YVO_4-Nd:YVO_4 laser with a pulse width of 2.5 ns and a pulse energy of 0.75 mJ at 2-kHz PRF.[20] By employing the same apparatus, Li *et al.*[21] and Zhang *et al.*[22]

*Project supported by the National Key Research and Development Program of China (Grant No. 2017YFB0405203) and the Shanxi "1331 Project" Key Subjects Construction, China (Grant No. 1331KSC).

†Corresponding author. E-mail: liyuanji@sxu.edu.cn

© 2020 Chinese Physical Society and IOP Publishing Ltd

built the pulse laser with a modified method called dual-loss-modulated simultaneously Q-switching and mode-locking, the PW of the 1-kHz pulse laser became as short as 339 ps, while the pulse energy was 0.38 mJ. However, there is no report on a single-cavity laser that can deliver a laser pulse train repeated in kHz level frequency with sub-ns PW and 1-mJ pulse energy by using the technique mentioned above, to the best of our knowledge.

In this paper, a novel method of achieving high energy sub-ns EO Q-switched lasers is proposed based on a detailed theoretical investigation on the laser behaviors. A sub-ns, 1-mJ level EO Q-switched TEM_{00} laser with a common cavity length and a moderate output transmission is built up after a series of experimental optimizations.

2. Theoretical analysis of EO Q-switched laser

2.1. Rate equations

The rate equations of a four-level Q-switched laser system can be written as[23]

$$\mathrm{d}n/\mathrm{d}t = -\gamma nc\sigma_{\mathrm{se}}\phi, \tag{1}$$

$$\mathrm{d}\phi/\mathrm{d}t = nc\sigma_{\mathrm{se}}\phi l/l_{\mathrm{c}} - \phi c\varepsilon/(2l_{\mathrm{c}}), \tag{2}$$

where n and ϕ are the population inversion density and photon density, respectively, γ is the inversion reduction factor, c is the light speed in vacuum, σ_{se} is the stimulated emission cross-section of gain medium at the laser wavelength, $l = 8$ mm and $l_{\mathrm{c}} = 72$ mm are the geometric length of the gain medium and the optical length of laser cavity, respectively, and ε is the loss factor per round trip.

To solve the rate equations, the pump pulse is assumed to be in an identical square-wave shape for simplicity, and the initial values of n and ϕ are given with the consideration that the rising edge (initial time) of the Q switching appears after the end of the falling edge of the pump pulse with a time delay of Δt:

$$n_0 = \frac{P_{\mathrm{in}}\tau_{\mathrm{f}}[1-\exp(-\alpha l)]}{h\nu_{\mathrm{p}}}\left[1-\exp\left(-\frac{T_{\mathrm{p}}}{\tau_{\mathrm{f}}}\right)\right]\frac{\omega_{\mathrm{l}}^2}{\omega_{\mathrm{pa}}^2}\frac{1}{\pi\omega_{\mathrm{pa}}^2 l}, \tag{3}$$

$$\phi_0 = n_0\frac{l}{c\tau_{\mathrm{f}}}\frac{\mathrm{d}\Omega}{4\pi}\exp\left(\frac{\Delta t}{\tau_{\mathrm{f}}}\right), \tag{4}$$

where P_{in} is the incident pump power, τ_{f} is the fluorescence lifetime of Nd:YVO_4 crystal, α is the pump absorption coefficient, $h\nu_{\mathrm{p}}$ is the energy of pump photon, T_{p} is the pump pulse width, ω_{pa} and ω_{l} are the average beam radii of pump and laser beams inside the laser crystal, respectively, $\mathrm{d}\Omega$ represents the solid angle of spontaneous emission that makes contribution to the stimulated emission.

2.2. Influence of loss parameters

Generally, ε is comprised of the dissipative loss (δ_0, set as 1% in simulation), the transmission of output coupler (T_{oc}, set as 60% in simulation), and the time-dependent loss of Q-switch (δ_{QS}).

In an EO Q-switched laser with the cavity-Q switched at rising edge of the PC driving signal, δ_{QS} is just the equivalent transmission at the polarizer and can be read as

$$\delta_{\mathrm{QS}}(t) = \cos^2\left(\frac{\pi}{2}\frac{V(t)}{V_{\lambda/4}}\right), \tag{5}$$

where $V_{\lambda/4}$ indicates the quarter wave voltage of PC, $V(t)$ is the driving signal sent to PC with a high-level voltage of V_{hl}, the normalized driving signal $(V(t)/V_{\lambda/4})$ can be assumed to be a super-Gaussian function.

$$\frac{V(t)}{V_{\lambda/4}} = \frac{V_{\mathrm{hl}}}{V_{\lambda/4}}\left(1-\exp\left[-\left(\frac{t}{t_{\mathrm{qr}}}\right)^4\right]\right)^4 \times \exp\left[-\left(\frac{t-t_{\mathrm{qs}}/2}{t_{\mathrm{qs}}}\right)^{400}\right], \tag{6}$$

where t_{qr} is the rise time of the driving signal, and t_{qs} is a constant determined by the duration of $V(t) = V_{\mathrm{hl}}$.

In common cases, the EO Q-switched laser is controlled by a driving signal with V_{hl} equal to $V_{\lambda/4}$. A typical normalized signal provided by a commercially available PC driver (Eksma Co Ltd, Model: PCD-UHR1-400-1.5) is recorded by a digital oscilloscope (Tektronix, DPO7254) and given by solid curve in Fig. 1. The dashed curve in Fig. 1, which is the simulated driving signal as a function of t, fits well with the measured signal by using Eq. (6) and setting $t_{\mathrm{qr}} = 4$ ns, $t_{\mathrm{qs}} = 160$ ns, and $V_{\mathrm{hl}} = V_{\lambda/4}$. The dotted curve in Fig. 1 represents the simulated driving signal as a function of t with the same settings except $V_{\mathrm{hl}} = 1.6V_{\lambda/4}$.

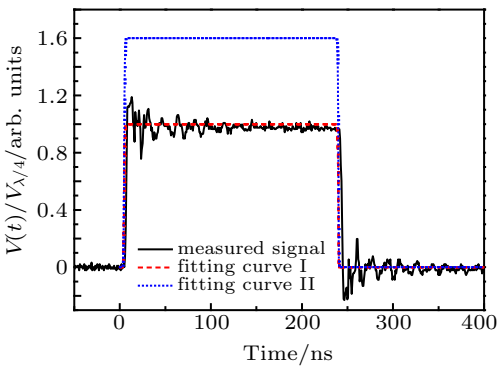


Fig. 1. Driving signal of Pockels cell, where solid curve denotes measured data, and dashed and dotted curve refer to simulated results from Eq. (6).

Using Eqs. (1)–(6) and the following parameters: $P_{\mathrm{in}} = 20$ W, $\sigma_{\mathrm{se}} = 17.5\times10^{-19}$ cm^2, $a = 10$ cm^{-1}, $\tau_{\mathrm{f}} = 98.42$ μs, $T_{\mathrm{p}} = 250$ μs, $\Delta t = 0$, $\gamma = 0.66$, $\omega_{\mathrm{pa}} = 290$ μm, $\omega_{\mathrm{l}} = 230$ μm, and $\mathrm{d}\Omega = 1$ mrad, the relations of the normalized laser intensity to time (t) at different values of V_{hl} are simulated and shown in Fig. 2. It is apparent that the driving signal with $V_{\mathrm{hl}} = V_{\lambda/4}$ is not the best choice. The laser pulse shape presents a relatively wide falling edge and the simulated pulse

width of laser is 1.02 ns. For $V_{\lambda/4} < V_{\rm hl} \leq 1.4V_{\lambda/4}$, the pulse width of laser is found to be narrowed with $V_{\rm hl}$ increasing, and reaches 0.98 ns at $V_{\rm hl} = 1.4V_{\lambda/4}$. However, if $V_{\rm hl}$ further increases to a value higher than $1.6V_{\lambda/4}$, the significant broadening of the rising and falling edges will lead the laser pulse width to increase.

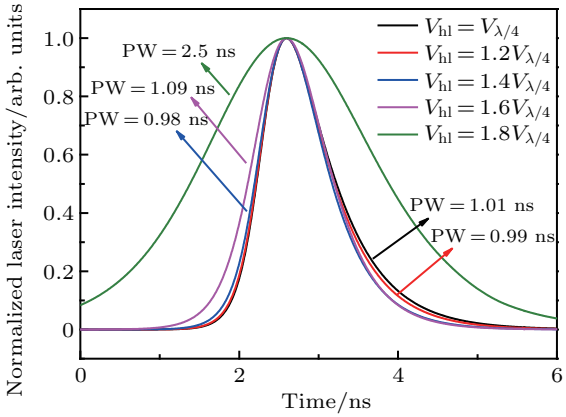


Fig. 2. Simulated pulse shapes of an EO Q-switched laser at different values of $V_{\rm hl}$.

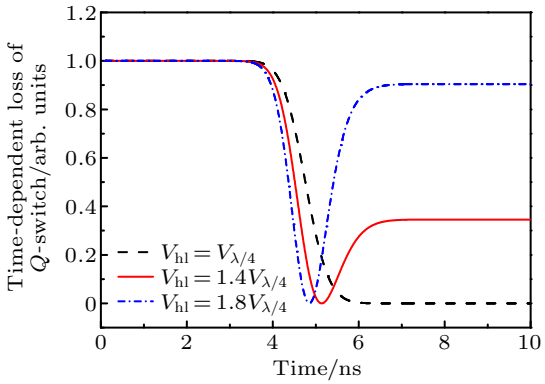


Fig. 3. Time-dependent losses of Q-switch at different values of $V_{\rm hl}$.

To understand the pulse shape variations of lasers shown in Fig. 2, the time-dependent losses of Q-switch as a function of time at $V_{\rm hl} = V_{\lambda/4}$, $1.4V_{\lambda/4}$, and $1.8V_{\lambda/4}$ are calculated, and the results are shown in Fig. 3. It can be seen that when the Q-switched laser is operated in the "common mode", *i.e.*, $V_{\rm hl} = V_{\lambda/4}$, the loss decline from 1 to 0 is finished in a duration of 2.3 ns and the "zero-loss" state lasts nearly 240 ns. Since the transmission of OC is 60% in our investigation, 40% of the laser photons generated during the Q-switching process will be reflected back into the cavity, leading to a wide falling edge. By contrast, when a driving signal with $V_{\rm hl} = 1.4V_{\lambda/4}$ is sent to PC, the loss decline from 1 to 0 is finished in a duration of 1.5 ns, and another process that $\delta_{\rm QS}$ rises from 0 to 0.34 in a duration of 1.3 ns takes place immediately. Hence, a portion of the laser photons reflected back into the cavity will no longer circulate in the cavity, but be coupled out at the polarizer. However, when the value of $V_{\rm hl}$ is higher than $1.6V_{\lambda/4}$, *e.g.*, $1.8V_{\lambda/4}$, another mechanism is dominated. Since the duration of the loss decline is further shortened and the value of $\delta_{\rm QS}$ at the final state is raised up to 0.9, the build-up process of the laser pulse is disturbed. Due to the low gain-to-loss ratio,[24] the buildup time of the laser pulse will increase and both the rising edge and the falling edge of the laser pulse will be broadened with $V_{\rm hl}$ increasing. From theoretical simulations, it can be concluded that the optimizing of the high-level voltage of the driving signal sent to PC is a convenient and feasible method to narrow and adjust the pulse width of an EO Q-switched laser with a common cavity length and a moderate output transmission.

2.3. Influence of doping concentration

To optimize the doping concentration ($C_{\rm d}$, in units of atomic%) of the gain medium, the $C_{\rm d}$-dependent spectroscopic parameters, such as the stimulated emission and absorption spectra, the fluorescence lifetimes of a series of Nd:YVO_4 crystals are determined. The absorption coefficient of Nd:YVO_4 crystal for a typical laser diode with a center wavelength of 808 nm can be given by[25]

$$\alpha = 20C_{\rm d} \quad (\rm cm^{-1}). \tag{7}$$

The fluorescence lifetime at 1064 nm as a function of $C_{\rm d}$ can be obtained by linear fitting of the data in Ref. [26]:

$$\tau_{\rm f} = -16.5C_{\rm d} + 106.67 \quad (\mu\rm s). \tag{8}$$

The stimulated emission at the laser wavelength of a series of Nd:YVO_4 crystal is measured experimentally by using an fluorescence spectrometer (Model: Omni-λ 3005, Omni-λ 500, Zolix).[27] Figure 4 shows the relationship between $\sigma_{\rm se}$ and $C_{\rm d}$ denoted by red spheres, and the black curve is the fitting by using a polynomial function as follows:

$$\begin{aligned}\sigma_{\rm se} \;=\; & 1.49082C_{\rm d}^3 - 10.28183C_{\rm d}^2 + 22.2149C_{\rm d} \\ & + 8.36075 \left(\times 10^{-23}\ \rm m^2\right). \end{aligned} \tag{9}$$

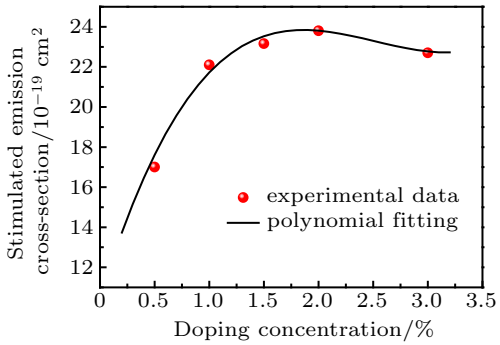


Fig. 4. Stimulated emission cross-section *versus* doping concentration at laser wavelength.

Using Eqs. (1)–(9) and setting $V_{\rm hl}/V_{\lambda/4}$ to be 1.4, the $C_{\rm d}$-dependent PW and pulse energy emitted from the output coupler are simulated respectively at incident pump power values of 20 W, 22.5 W, and 25 W, and the results are shown in Fig. 5. It can be seen that the favorite range of $C_{\rm d}$ corresponding to both narrow PW and high pulse energy is generally from 0.5%

to 1%. Moreover, when the pump power is below the thermal threshold that causes serious thermal effect, higher pump power is expected to be helpful in achieving the narrower PW and higher pulse energy.

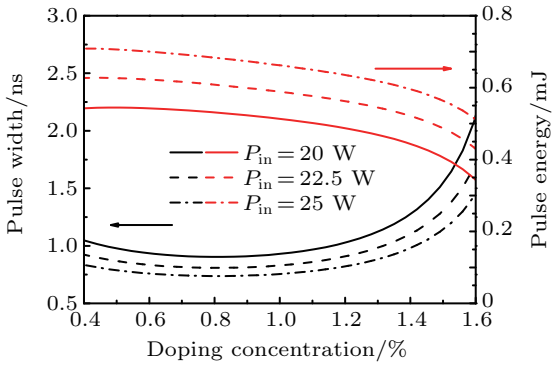


Fig. 5. Laser pulse width and pulse energy *versus* doping concentration.

3. Experimental setup and results

An EO Q-switched laser pumped by a laser-diode (LD) is fabricated as shown in Fig. 6. The pump laser provided by a commercially available laser diode (LIMO, Model: LIMO60-F400-DL808-EX1126) with a center wavelength of 808 nm is delivered into the gain medium through a fibre with a core diameter of 400 μm and a lens combination (F1, F2) with a magnification ratio of 4 : 5. The "L"-shape cavity is composed of two mirrors, a polarizer, a gain medium and an EO Q-switch. The input coupler is a volume Bragg grating (VBG) with a wavelength bandwidth of 0.3 nm and diffraction efficiency higher than 99.5% at 1064 nm. The OC is a concave mirror with a curvature radius of 1000 mm and partial reflection coating at 1064 nm ($R_{1064\ \mathrm{nm}} = 60\%$). The polarizer is a 45° thin film polarizer (TFP) with polarization distinction ratio higher than 1000 : 1. The gain medium is a composite a-cut Nd:YVO_4 crystal formed by an undoped end cap of 2 mm and a Nd-doped portion of 8 mm. During the experiment, three crystals with identical parameters except for the Nd^{3+} concentration are employed. Both end faces of the crystals are polished and anti-reflection coated at 808 nm and 1064 nm ($R_{808\ \mathrm{nm}} < 2\%$, $R_{1064\ \mathrm{nm}} < 0.2\%$). The Nd:$YVO_4$ crystal is mounted in a temperature controlled copper cooler 5 mm far from VBG, while the optical length of the cavity is 72 mm. The EO Q-switch, which consists of a QWP and a PC formed by a pair of thermally compensated $RbTiOPO_4$ (RTP) crystals, is positioned between TFP and OC. To overcome the thermal depolarization originating from the nonuniform pump and laser absorption of the two RTP crystals in the PC, the precise temperature control of the PC is also needed.[28] The PC with $V_{\lambda/4}$ of 860 V is driven by a commercial available high-voltage driver (Eksma, Model: PCD-UHR1-400-1.5) with a rise time of 4 ns. Note that a delay generator (SRS, Model: DG645) is employed to synchronize the PC driver and the pulsed current driver for the laser diode, both are operated at 1-kHz PRF.

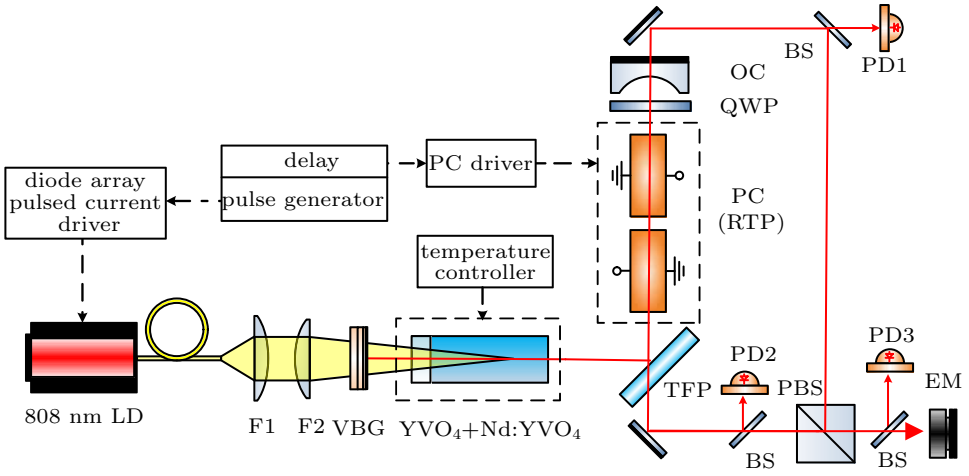


Fig. 6. Schematic diagram of EO Q-switched laser. VBG: volume Bragg grating; TFP: thin film polarizer; OC: output coupler; QWP: quarter wave plate; PC: Pockels cell; BS: beam splitter; PBS: polarization beam splitter; PD: photodiode; EM: energy meter.

Figure 7 shows the laser pulse shapes detected by three high speed photodetectors (PD1, PD2, PD3, Newport, Model: 818-BB-35) and recorded by an oscilloscope (Tektronix, Model: DPO7254) synchronously at an incident pump power of 25 W, pump duty cycle of 25%, and a doping concentration of 0.5 at.%. More specifically, figure 7(a) shows the pulse shape of output from OC when the laser is operated in the "traditional mode" and there is no output from TFP. Figures 7(b) and 7(c) display the pulse shapes of outputs from OC and TFP in the case of $V_{\mathrm{hl}} = 1.4V_{\lambda/4}$, respectively. Figure 7(d) shows the pulse shape of the combination of the two outputs detected by PD3. It can be seen that when the PC driving signal is modified by simply raising up V_{hl} from $V_{\lambda/4}$ to $1.4V_{\lambda/4}$, the PW of laser can be narrowed from 1.03 ns to 0.78 ns. It is worth noting that when the EO Q-switched laser is operated in this new mode, beside an s-polarized pulse laser coupled out from OC, a p-polarized pulse laser with almost identical pulse shape is coupled out from TFP simultaneously. A time

delay of 0.1 ns is observed between the start times of the two laser pulses. When the two pulse lasers are combined on a polarized beam splitter (PBS) with the time delay being compensated, the recorded pulse shape gives a PW of 0.78 ns, the pulse energy is measured by an energy meter (EM, Newport, Model: 1935-C) to be 890 μJ, while the energy of the laser operated in "traditional mode" is measured to be 1.1 mJ.

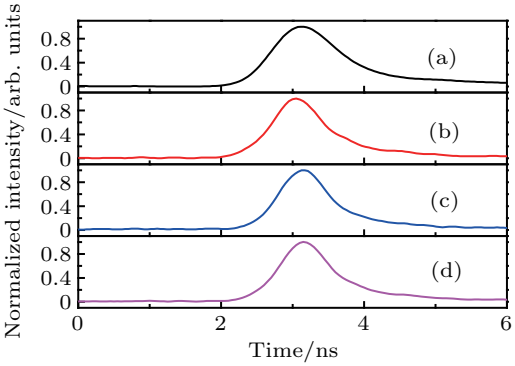


Fig. 7. Single pulse shapes at different values of $V_{\rm hl}$: (a) $V_{\rm hl} = V_{\lambda/4}$, (b) laser from OC at $V_{\rm hl} = 1.4V_{\lambda/4}$, (c) laser from TFP at $V_{\rm hl} = 1.4V_{\lambda/4}$, (d) combination of the laser from OC and TFP at $V_{\rm hl} = 1.4V_{\lambda/4}$.

The continuous tuning of the PW and pulse energy of the laser combinations under 25-W pumping is also demonstrated by varying the value of $V_{\rm hl}/V_{\lambda/4}$, and the results are shown in Figs. 8(a) and 8(b). Three gain media with the doping concentrations of 0.5 at.%, 0.7 at.%, and 1 at.% are chosen according to the simulation results in Fig. 5. The measured data corresponding to the three doping concentrations are denoted by balls, squares and triangles, respectively. The theoretical predictions corresponding to the three doping concentrations are denoted by black, red, and blue curves, respectively. It can be seen that the dependence of laser PW or pulse energy on $V_{\rm hl}/V_{\lambda/4}$ shows the same tendencies in the three cases, and the theoretical predictions accord well with the measured data in a major part of the tuning range when the gain media with the doping concentrations of 0.5 at.% and 0.7 at.% are used. However, the experimental results corresponding to $C_{\rm d} = 1$ deviate significantly from the theoretical predictions, and this phenomenon may be caused by the serious thermal effect since the measured thermal focal length of the gain medium with a doping concentration of 1 at.% is much shorter than those of the other two gain media. In the three cases, the PWs always vary slowly in the range of $V_{\rm hl}/V_{\lambda/4}$ from 1 to 1.5, but rise up steeply in a range of $V_{\rm hl}/V_{\lambda/4}$ from 1.5 to 1.8. Consequently, when the EO Q-switched laser is operated with varying $V_{\rm hl}/V_{\lambda/4}$, the PW of laser is not only narrowed significantly, but also adjustable. For example, it can be adjust from 0.78 ns to 1.3 ns when the gain medium with the doping concentration of 0.5 at.% is used. Note also that the narrowest PW of 0.73 ns is achieved when $V_{\rm hl}/V_{\lambda/4}$ is set to be 1.4 and the gain medium with a doping concentration of 0.7 at.% is used. Moreover, when the value of $V_{\rm hl}/V_{\lambda/4}$ varies from 1 to 1.8, the pulse energy always decreases monotonically.

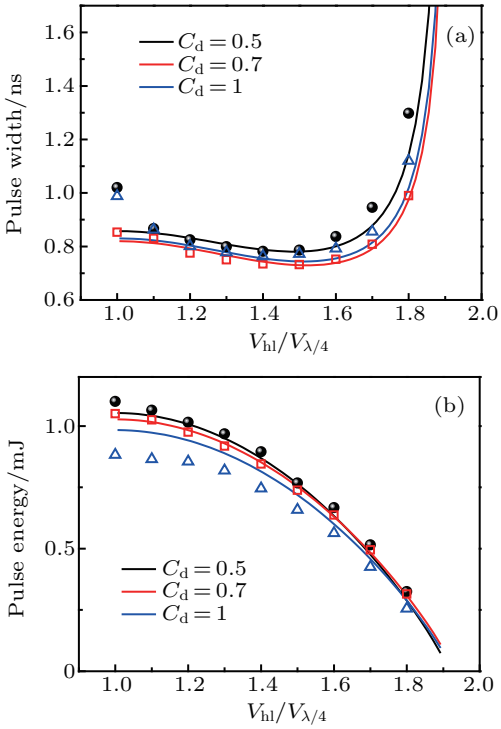


Fig. 8. (a) Pulse width and (b) pulse energy of pulse laser combination *versus* $V_{\rm hl}/V_{\lambda/4}$ for three different values of $C_{\rm d}$.

To balance the narrow PW and high pulse energy, the optimal design is implemented by using the gain medium with a doping concentration of 0.7 at.% and setting $V_{\rm hl}/V_{\lambda/4}$ to be 1.2. And in this case, the PW and pulse energy of the laser are 0.77 ns and 1.04 mJ, respectively. The beam qualities of the sub-ns laser are also measured by using a laser beam analyser (Spricon, Model: M2-200-BB; CCD: GRAS-20S4M-C), and the results are shown in Fig. 9. The beam quality of the laser combination is $M_x^2 = 1.26$ along the horizontal direction and $M_y^2 = 1.32$ along the vertical direction at the output energy of 1.04 mJ.

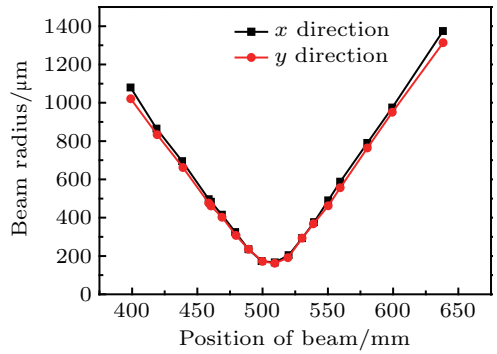


Fig. 9. Plots of measured beam radius *versus* beam position in x and y directions for the combination of pulse lasers.

4. Conclusions

In this work, we investigated the influences of the driving signal sent to PC and the doping concentration of the gain medium on the performance of an EO Q-switched laser numerically and experimentally. Both the numerical simulations and the experimental results reveal a fact that the traditionally used

high-level-voltage of the driving signal (V_{hl}), which equals the quarter wave voltage of PC, is not the best choice for its corresponding laser pulse shape presenting a relatively wide falling edge. When a driving signal with an approximate square wave shape and theoretically determined optimal V_{hl} is applied to a PC mounted in an EO Q-switched laser and a gain medium with an optimal doping concentration is employed, significant compression of laser PW is observed as expected. It is also found that in this new operation mode, the s-polarized laser coupled out from OC and the p-polarized laser coupled out from TFP have almost identical pulse shapes. When the two lasers are combined with the time delay being compensated, a stable TEM_{00} laser source with PRF of 1 kHz, PW of 0.77 ns, and pulse energy of 1.04 mJ is realized. Moreover, by tuning the value of V_{hl}, the laser PW can be precisely and quickly adjusted in a certain range. This kind of high energy sub-ns EO Q-switched laser has the advantages of low-cost, low energy-consumption, high stability and reliability, easy-to-be-synchronized with the other detectors. As a consequence, it promises to have applications in the fields of satellite-based ranging and imaging, outdoors measurement like vehicle lidar, *etc*.

References

[1] Markus T, Neumann T, Martino A, Abdalati W, Brunt K, Csatho B, Farrell S, Fricker H, Gardner A, Harding D, Jasinski M, Kwok R, Magruder L, Lubin D, Luthcke S, Morison J, Nelson R, Neuenschwander A, Palm S, Popescu S, Shum C K, Schutz B E, Smith B, Yangak Y K and Zwallya J 2017 *Remote Sens. Environ.* **190** 260

[2] Steven R T, Dexter A and Bunch J 2016 *Methods* **104** 101

[3] Chambonneau M, Li Q, Chanal M, Sanner N and Grojo D 2016 *Opt. Lett.* **41** 4875

[4] Ishizuki H and Taira T 2017 *Opt. Express* **25** 2369

[5] Lim H H and Taira T 2017 *Opt. Express* **25** 6302

[6] Demos S G, Negres R A, Raman R N, Shen N, Rubenchik A M and Matthews M J 2016 *Opt. Express* **24** 7792

[7] Zhang L H, Sun L J and Ma X H 2013 *Laser Phys. Lett.* **10** 055601

[8] James J, Murukeshan V M, Sathiyamoorthy K and Woh L S 2014 *Laser Phys.* **24** 085608

[9] Zou Y, Hui Y L, Cai J L, Guo N, Jiang M H, Lei H and Li Q 2017 *Chin. Phys. B* **26** 094206

[10] Deyra L, Martial I, Balembois F, Diderjean J and Georges P 2013 *Appl. Phys. B* **111** 573

[11] Lin Y N, Fang W T, Gu C and Xu L X 2016 *Chin. Phys. Lett.* **33** 054203

[12] Zhang L, Zhang D and Li J Z 2013 *Chin. Phys. B* **22** 074207

[13] Zayhowski J J and Dill C 1995 *Opt. Lett.* **20** 716

[14] Horiuchi R, Adachi K, Watanabe G, Tei K and Yamaguchi S 2008 *Opt. Express* **16** 16729

[15] Liu Q, Meng J Q, Zu J F, Jiang J, Chen S L and Chen W B 2017 *Chin. J. Lasers* **44** 0601005 (in Chinese)

[16] Chen X Y, Wu J, Wu C T, Sun H T, Yu Y J and Jin G Y 2015 *Laser Phys.* **25** 045003

[17] Yin X L, Jiang M H, Sun Z, Hui Y L, Lei H and Li Q 2017 *Appl. Opt.* **56** 2893

[18] McDonagh L, Wallenstein R and Knappe R 2006 *Opt. Lett.* **31** 3303

[19] Liu K, He L J, Bo Y, Wang X J, Shen Y, Liu Z, Yuan L, Peng Q J, Cui D F and Xu Z Y 2017 *Opt. Lett.* **42** 2467

[20] Li T, Zhao S Z, Zhuo Z, Yang K J, Li G Q and Li D C 2009 *J. Opt. Soc. Am. B* **26** 1146

[21] Li S X, Li D C, Zhao S Z, Li G Q, Li X Y and Qiao B 2016 *Opt. Express* **24** 4022

[22] Zhang H J, Zhao S Z, Yang K J, Li G Q, Li D C, Zhao J and Wang Y G 2013 *Appl. Opt.* **52** 6776

[23] Coyle D B, Guerra D V and Kay R B 1995 *J. Phys. D* **28** 452

[24] Degnan J J 1989 *IEEE J. Quantum Electron.* **25** 214

[25] Chen Y F, Lee L J, Huang T M and Wang C L 1999 *Opt. Commun.* **163** 198

[26] Mukhopadhyay P K, George J, Sharma S K, Ranganathan K and Nathan T P S 2002 *Opt. Laser Technol.* **34** 357

[27] Turri G, Jenssen H P, Cornacchia F, Tonelli M and Bass M 2009 *J. Opt. Soc. Am. B* **26** 2084

[28] Zhao X, Li Y J, Feng J X and Zhang K S 2017 *Chin. J. Lasers* **44** 0501006 (in Chinese)